Naturwissenschaften (2008) 95:1079–1083
DOI 10.1007/s00114-008-0419-3

SHORT COMMUNICATION

Virtual cranial endocast of the oldest giant panda (*Ailuropoda microta*) reveals great similarity to that of its extant relative

Wei Dong

Received: 27 January 2008 / Revised: 3 June 2008 / Accepted: 4 June 2008 / Published online: 4 July 2008
© Springer-Verlag 2008

Abstract Recent development of computed tomography and three-dimensional visualization techniques has enabled the non-destructive inspection of the endocast morphology of fossil neurocranium, the basic material for paleoneurological study. A virtual cranial endocast was reconstructed based on the first skull of the oldest giant panda, *Ailuropoda microta*, discovered recently and dated at more than 2 Myr (million years) ago. It was compared with that of the extant giant panda (*A. melanoleuca*) and that of the polar bear (*Ursus maritimus*), as well as CT slices of the late Pleistocene *A. baconi*. The overall endocast morphology of *A. microta* is more similar to that of *A. baconi* and *A. melanoleuca* than to that of *U. maritimus*. The absolute endocast size is the smallest in *A. microta*, largest in *A. baconi*, and intermediate in *A. melanoleuca*. However, the proportion of cerebral volume to total endocast size is very close to each other between the oldest and extant giant panda, as well as the sulcal length per unit area of cerebral endocast surface.

Keywords Giant panda · Paleoneurology · Evolution · Computed tomography · Plio–Pleistocene

Introduction

The rarity of natural fossil cranial endocasts as well as avoidance of destructive dissection on precious skulls often hinders paleoneurological research. With the development of computed tomography (CT) and three-dimensional visualization techniques, it becomes more and more practical for paleontologists to carry out noninvasive dissection on rare and precious fossil skulls to learn endocast morphology and undertake quantitative analyses (Zollikofer and Ponce de León 2000; Falk et al. 2005; Vialet et al. 2005; Macrini et al. 2006; Dong et al. 2007).

The extant giant panda, *Ailuropoda melanoleuca*, is geographically restricted in central China as an endangered species (Nowak and Paradiso 1983; Wang 2003), but its Plio–Pleistocene relative, known as *A. microta*, had a larger geographic range from central to southern China, and the late Pleistocene giant panda, known as *A. baconi*, had an even larger range from northern China to Southeast Asia (Colbert and Hooijer 1953; Huang 1993; Jin et al. 2007). Previous research on fossil giant pandas was largely based on dental characters from numerous teeth of different species and limited to external cranial characters from a few precious skulls of *A. baconi* (Colbert and Hooijer 1953; Pei 1987; Huang 1993). The newly discovered first skull of the oldest giant panda (*A. microta*) from Leye of Guangxi in southern China (Jin et al. 2007), together with a skull of the late Pleistocene giant panda from Liujiang Man Site of

Electronic supplementary material The online version of this article (doi:10.1007/s00114-008-0419-3) contains supplementary material, which is available to authorized users.

W. Dong (✉)
Institute of Vertebrate Paleontology and Paleoanthropology,
Chinese Academy of Sciences,
Beijing 100044, China
e-mail: dongwei@ivpp.ac.cn

W. Dong
National Laboratory of Pattern Recognition,
Institute of Automation, Chinese Academy of Sciences,
Beijing 100080, China

Guangxi (Pei 1987), allows us to explore the unknown endocast morphology of fossil giant pandas and to learn their evolution by noninvasive means.

Materials and methods

The main material is a skull of *A. microta* (IVPP V14564), dated at more than 2 Myr ago. The comparative materials are a skull of the late Pleistocene giant panda, *A. baconi* (IVPP V5038), dated at about 0.1 Myr, a skull of the extant giant panda, *A. melanoleuca* (IVPP 1236), and a skull of the extant polar bear, *Ursus maritimus* (IVPP 50). The skulls are well preserved except that of *A. baconi* which is broken in the region between the frontal and parietal bones (Fig. 1, second column). Judged by the fully emerged permanent dentition, the skulls are all from adults.

The skulls were scanned with a high-resolution medical CT scanner Lightspeed VCT manufactured by GE Medical Systems and installed at the Renmin Hospital of Peking University. The scanning direction was coronal (transverse), with a slice interval of 0.625 mm, slice thickness of 0.5 mm, X-ray tube voltage 120 kV, tube current 200 mA for fossil skulls, and 190 mA for extant skulls. Two-dimensional slice images were generated by the scanner with LightSpeedApps (version 06MW03.4) according to protocol 1.1 Routine Head sec. All slices were formatted in the same size of 512×512 pixels and color depth of 16 bits. The reconstruction diameter and pixel resolution were 156.6936 mm and 0.306641 mm for *A. microta*, 251.508 mm and 0.492188 mm for *A. baconi*,

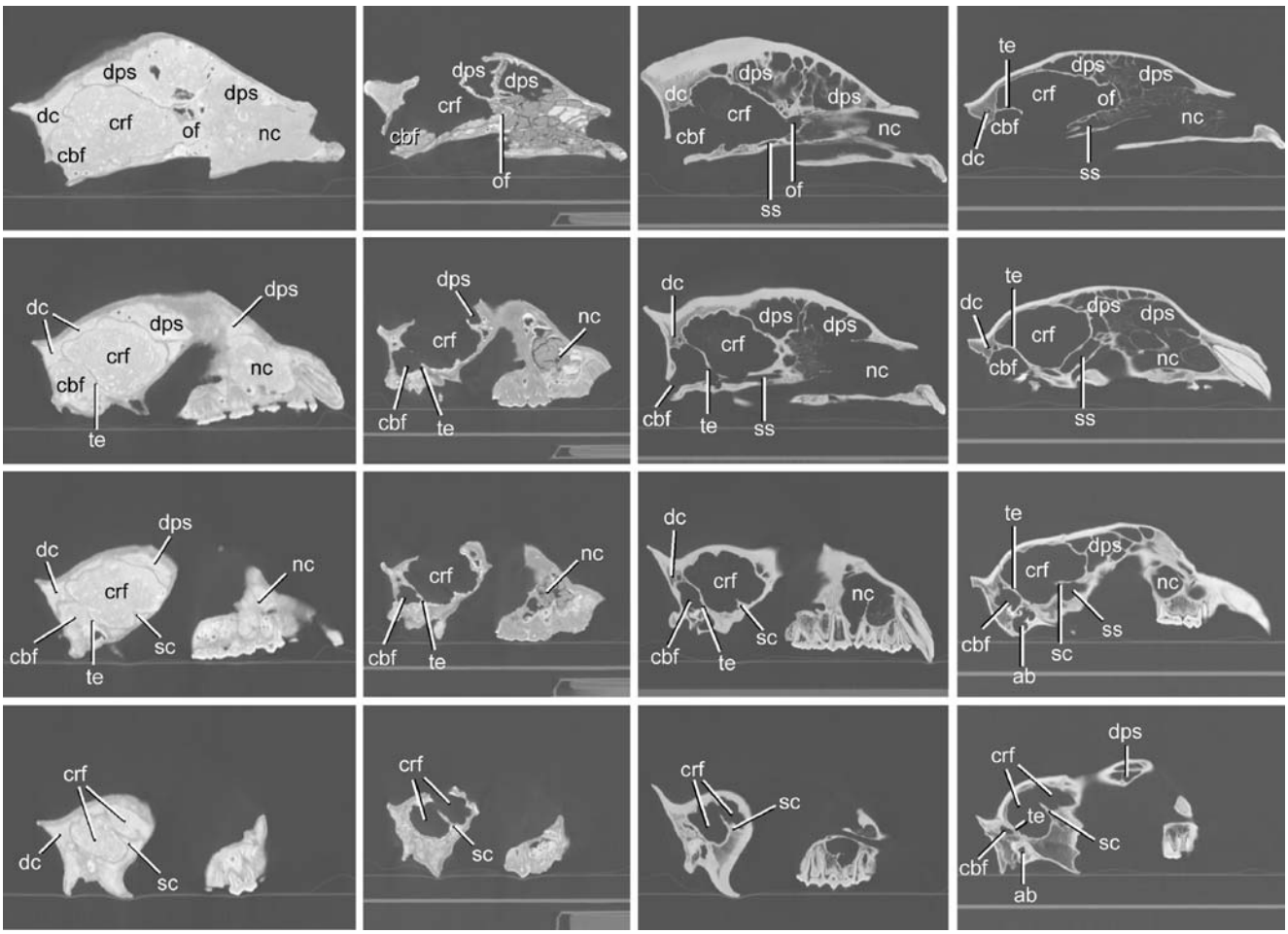

Fig. 1 Comparison of reconstructed sagittal slices of different skulls. From the first to fourth column: *A. microta* (slice size 156.6936× 247.5 mm), *A. baconi* (slice size 251.508×298.75 mm), *A. melanoleuca* (slice size 207.594×288.125 mm), and *Ursus maritimus* (slice size 198.6114×293.125 mm); from the first to the fourth line: from medial sagittal section to lateral one. *cbf*, cerebellar fossa; *crf*, cerebral fossa; *dc*, diploe of calvaria; *dps*, dorsal paranasal sinuses; *nc*, nasal cavity; *of*, olfactory fossa; *sc*, sylvius crest (perpendicular crest); *ss*, sphenoid sinus; *te*, tentorium

207.594 mm and 0.40625 mm for *A. melanoleuca*, and 198.6114 mm and 0.388672 mm for *U. maritimus*.

The segmentation, extraction, and measurement of cranial endocasts were carried out with Amira (version 3.1.1 and 4.0.1) from Mercury (http://www.mc.com/tgs). The measurement of endocranial volume was based on the statistics of all segmented pixels on each CT slice, slice interval, and the number of segmented slices. The measurement of endocranial surface area was based on the statistics of triangles on the mesh generated from the segmented cranial endocasts by Amira. Sulcal length was measured directly on the virtual cranial endocasts with the three-dimensional ruler tool of Amira.

The boundary between the olfactory fossa and cerebral fossa was defined by the cross section in the middle of the ridge between these fossae. The boundary between the cerebral fossa and cerebellar fossa was defined by the tentorium and its extension across the endocranial cavity. The anatomical features of the extracted endocasts are labeled following the brain terminology of Pirlot et al. (1985).

Results

I first explored scanned CT data, i.e., coronal slices, and then the reconstructed sagittal and axial slices. The slices in three dimensions show that the internal cranial osteology of *A. microta* is surprisingly well preserved (Fig. 1, first column) and that the endocranial cavity, although filled with geological matrix, can be clearly segmented and extracted (Fig. 2, middle column; Figs. S1, S2, S3, S4 show different views of the extracted virtual cranial endocast), whereas the endocranial cavity of *A. baconi* is not well preserved (Fig. 1, second column) and its endocranial cavity can only be segmented by estimating the missing boundaries of the endocranial cavity between the parietals and frontals. The endocast morphology of the two extant specimens is logically very clear (Fig. 1, third and fourth columns) and was easily segmented and extracted (Fig. 2, lateral columns). The osseous tentorium separating the cerebral fossa and cerebellar fossa is very clear in both the fossil and extant specimens. The boundary between the olfactory fossa and cerebral fossa is also clear in all specimens.

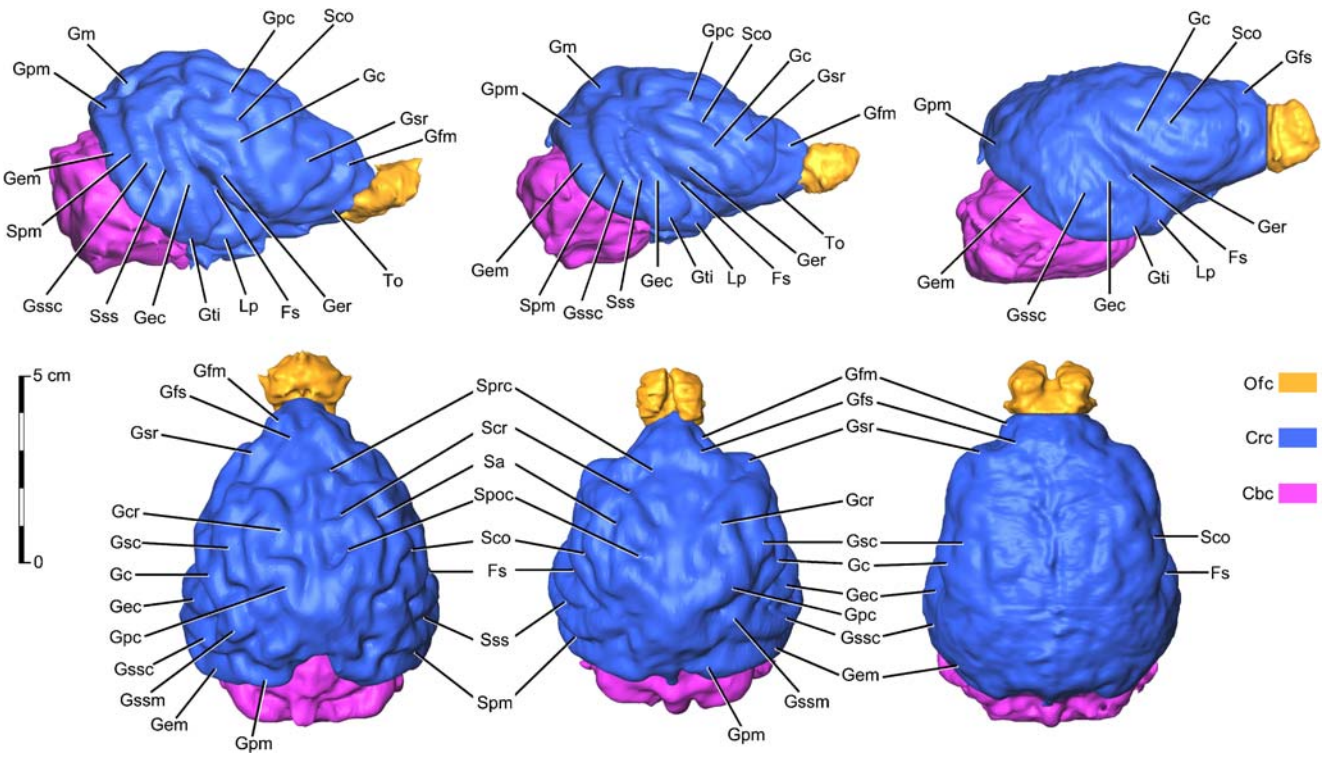

Fig. 2 Lateral (*upper line*) and dorsal (*lower line*) comparison of cranial endocasts of *A. melanoleuca* (*left column*), *A. microta* (*middle column*), and *U. maritimus* (*right column*). *Cbc*, cerebellar fossa endocast; *Crc*, cerebral fossa endocast; *Fs*, fissura sylvius; *Gc*, gyrus coronalis; *Gcr*, gyrus cruciatus; *Gec*, gyrus ectosylvius caudalis; *Gem*, gyrus ectomarginalis; *Ger*, gyrus ectosylvius rostralis; *Gfm*, gyrus frontalis medius; *Gfs*, gyrus frontalis superior; *Gm*, gyrus marginalis; *Gpc*, gyrus postcruciatus; *Gpm*, gyrus postmarginalis; *Gsc*, gyrus sigmoidea caudalis; *Gsr*, gyrus sigmoidea rostralis; *Gssc*, gyrus suprasylvius caudalis; *Gssm*, gyrus suprasylvius medius; *Gti*, gyrus temporalis inferior; *Lp*, lobus piriformis; *Ofc*, olfactory fossa endocast; *Sa*, sulcus ansatus; *Sco*, sulcus coronalis; *Scr*, sulcus cruciatus; *Spoc*, sulcus postcruciatus; *Spm*, sulcus postmarginalis; *Sprc*, sulcus precruciatus; *Sss*, sulcus suprasylvius; *To*, tractus olfactorius

The overall endocast morphology of the three giant pandas is very similar, but different from that of the polar bear (Figs. 1 and 2). The cerebral sulcus and gyrus casts on the surface of the cerebral fossa are well defined in the giant pandas but faint in the polar bear. On the contrary, blood vessel casts are more evident in the polar bear. The tentorium inclines sharply downwards in giant pandas but gently downwards in polar bear (Fig. 1).

Measurements from the endocasts are listed in Table 1.

Within *Ailuropoda*, the absolute size of the cerebral endocast is the most similar between *A. microta* and *A. melanoleuca* (Table 1). The cerebral endocast volume of *A. melanoleuca* is nearly identical to that of *U. maritimus*. But the proportion of cerebral volume to the total endocast size is very similar among the three species of *Ailuropoda* compared with that of *U. maritimus* (Table 1). The sulcal length per unit area of the cerebral surface is most similar between *A. microta* and *A. melanoleuca*. The absolute sizes of the cerebellar endocasts from the smallest to the largest are *A. microta*, *A. melanoleuca*, *U. maritimus*, and *A. baconi* (Table 1). The proportion of cerebellar volume to total endocast volume is most similar among the giant pandas compared with that of the polar bear. The olfactory endocast is larger and thicker, but shorter in *U. maritimus* compared with that of *Ailuropoda* (Table 1, Fig. 2).

Discussion

Cranial endocasts are reflections of the internal surfaces of braincase bones and indicate the partial variability of brain features instead of the original brain structures themselves. The internal bones show molds of meninges (including the outermost dura mater) along with dural sinuses and cisterns occupying the space between the skull bones and the brain. These soft tissue structures can obscure features of the brain on the corresponding endocast. Nonetheless, anatomic and metric data obtained from the endocasts in this paper allow us to study the brain morphology and evolution of the giant pandas. The sulci are wide on the brain of *A. melanoleuca* (Xie and Jiao 1986) allowing the dura mater to closely follow the contours of the valleys. That explains the well-developed gyri and sulci on the virtual cranial endocast of *A. melanoleuca*. Correspondingly, the developed gyri and sulci on the virtual endocast of *A. microta* imply the existence of wide sulci on the corresponding brain. On the contrary, the sulci on the natural brain specimen of *U. maritimus* are less wide (Welker et al. 2008), and consequently the gyri and sulci on its virtual endocast are not well developed.

The body and brain sizes implied from endocasts of the Plio–Pleistocene *A. microta* are the smallest of the giant pandas, whereas those of the late Pleistocene *A. baconi* are the largest. It is remarkable that the brain size of the giant pandas increased from the Plio–Pleistocene to the late Pleistocene and decreased since the end of the late Pleistocene (Table 1, Table 1 in Jin et al. 2007).

A decrease in brain size is also observed in human evolution after the emergence of anatomically modern humans corresponding to a generalized gracilization of the body structures (Ruff et al. 1997; Bruner 2003) as well as in domesticated mammals (Kruska 1988, 2005). Although *A. melanoleuca* does not look gracile, it is "gracile" compared with the polar bear. Both have similar-sized cranial endocasts but the former has a much smaller body size than the latter (Nowak and Paradiso 1983). Mosaic brain organization within orders is thought to be caused by selective adaptation (de Winter and Oxnard 2001; Kruska 1987, 2005), and the different patterns of endocast morphology between giant pandas and the polar bear can therefore be considered as the result of such evolution.

Table 1 Cranial endocast measurements and comparison of the giant pandas and the polar bear

	A. microta	*A. baconi*	*A. melanoleuca*	*U. maritimus*
Cerebral volume (ml)	163.62	332.73[a]	217.03	215.55
Proportion of cerebral volume to total endocast volume (%)	77.60	76.68	78.44	74.58
Cerebral surface area (cm^2)	193.34	292.09[a]	239.39	218.78
Total sulcus length (cm)	99.18	–	125.12	–
Sulcal length per unit area (cm^{-1})	0.513	–	0.523	–
Cerebellar volume (ml)	43.10	95.26[a]	54.80	66.85
Proportion of cerebellar volume to total endocast volume (%)	20.45	21.95	19.81	23.13
Cerebellar surface area (cm^2)	71.01	122.22[a]	88.95	96.93
Olfactory volume (ml)	3.77	5.95	4.86	6.62
Proportion of olfactory volume to total endocast volume (%)	1.79	1.37	1.76	2.29
Olfactory surface area (cm^2)	15.24	18.58	17.20	22.59
Total endocast volume (ml)	210.85	433.94	276.69	289.02

[a] Value based on endocast with estimated dorsal boundaries due to broken state of skull (IVPP V5038) between frontals and parietals (see Fig. 1)

Acknowledgement The author would like to thank Drs. Jin and Liu for providing the skull of *A. microta*, Dr. Zhu for scanning the skulls, and Prof. D. Kruska for providing some useful reprints. The author would also like to acknowledge three referees for critiques and suggestions to improve the manuscript. The present work was supported by the Chinese National Natural Science Foundation (Project No. 40772014) and Knowledge Innovation Program of Chinese Academy of Sciences (No. KZCX2-YW-106).

References

Bruner E (2003) Fossil traces of the human thought: paleoneurology and the evolution of the genus *Homo*. J Anthropol Sci 81:29–56

Colbert EH, Hooijer DA (1953) Pleistocene mammals from the limestone fissures of Szechuan, China. Bull Am Mus Nat Hist 102:1–134

de Winter W, Oxnard CE (2001) Evolutionary radiations and convergences in the structural organization of mammalian brains. Nature 409:710–714

Dong W, Hou X, Liu J, Fang Y, Jin C, Zhu Q (2007) 3D virtual reconstruction of the Pleistocene cheetah skull from the Tangshan, Nanjing, China. Progr Nat Sci 17:74–79

Falk D, Hildebolt C, Smith K, Morwood MJ, Sutikna T, Brown P, Jatmiko E, Saptomo EW, Brunsden B, Prior F (2005) The brain of LB1, *Homo floresiensis*. Science 308:242–245

Huang WP (1993) The skull, mandible and dentition of giant pandas (*Ailuropoda*): morphological characters and their evolutionary implications. Vertebrata Pal Asiatica 31:191–207

Jin C, Ciochon RL, Dong W, Hunt RM Jr, Liu J, Jaeger M, Zhu Q (2007) The first skull of the earliest giant panda. Proc Natl Acad Sci USA 104:10932–10937

Kruska D (1987) How fast can total brain size change in mammals. Hirnforsch 28:59–70

Kruska D (1988) Mammalian domestication and its effect on brain structure and behavior. In: Jerison HJ, Jerison I (eds) The evolutionary biology of intelligence. Nato ASI series in Ecology G17. Springer, Heidelberg, pp 211–250

Kruska DCT (2005) On the evolutionary significance of encephalization in some eutherian mammals: effects of adaptive radiation, domestication, and feralization. Brain Behav Evol 65:73–108

Macrini TE, Rowe T, Archer M (2006) Description of a cranial endocast from a fossil platypus, *Obdurodon dicksoni* (Monotremata, Ornithorhynchidae), and the relevance of endocranial characters to monotreme monophyly. J Morphol 267:1000–1015

Nowak RM, Paradiso JL (1983) Walker's mammals of the world. The Johns Hopkins University Press, Baltimore

Pei WZ (1987) Carnivora, Proboscidea and Rodentia from Liucheng Gigantopithecus Cave and Other Caves in Guangxi. Mem Inst Vertebr Palaeont Palaeoanthrop, Acad Sinica 18:5–115

Pirlot P, Jiao S, Xie J (1985) The brain of the giant panda (*Ailuropoda*). Fortschr Zool 30:571–574

Ruff CB, Trinkaus E, Holliday TW (1997) Body mass and encephalization in Pleistocene *Homo*. Nature 387:173–176

Vialet A, Li T, Grimaud-Hervé D, de Lumley M-A, Liao M, Feng X (2005) Proposition de reconstitution du deuxième crâne d'*Homo erectus* de Yunxian (Chine). C R Palevol 4:265–274

Welker W, Johnson JI, Noe A (2008) Comparative mammalian brain collections. http://www.brainmuseum.org/, 10-Jan

Wang YX (2003) A complete checklist of mammal species in China—a taxonomic and geographic reference. China Forestry Publishing House, Beijing

Xie JQ, Jiao SS (1986) Brain. In: Beijing Zoo, Beijing University, Beijing Agricultural University (ed) Morphology of the giant panda—systematic anatomy and organ-history. Science Press, Beijing, pp 364–392

Zollikofer CPE, Ponce de León MS (2000) Computer-assisted paleoanthropology: methods, techniques and applications. Acta Anthropologica Sinica 19(Suppl):90–97